

Statistical Characterisation of Speckle in Clinical Echocardiographic Images with Pearson Family of Distributions

Abhinav Gupta*[‡] and Karmeshu*

*Jawaharlal Nehru University, New Delhi-110067, India

[‡]Jaypee Institute of Information Technology, Noida-201307, India

E-mail: abhinav.dsp@gmail.com

ABSTRACT

The statistical characterisation of gray level distribution of echocardiographic images is commonly done in terms of unimodal probability densities such as Rayleigh, Gamma, Weibull, Nakagami, and Lognormal. Amongst these distributions, the Gamma density is found to provide better empirical model that fits to real data sets. We propose to extend the class of probability distributions by exploring Pearson family to characterise blood and tissue in echocardiographic images. It is found that Pearson Type I characterises the tissue regions whereas Type I, Type IV and Type VI classify blood regions. The statistical measures viz. Jensen-Shannon (JS) divergence and Kolmogorov-Smirnov (KS) statistics reveal that Pearson family of curves outperforms the Gamma distribution.

Keywords: Speckle, echocardiography, Pearson distributions, tissue Characterisation.

1. INTRODUCTION

A major challenge in B-mode ultrasound (US) imaging is statistical characterisation of speckle¹⁻⁴ which is often regarded as containing information about the underlying tissue structure. The high order statistical measures provide information about texture of the speckle pattern, which depends on spatial distribution² of random scatterers. The speckle probability density at the transducer is transformed into speckle densities in the image through a chain of complex image processing steps, which are difficult to model mathematically³. In absence of the theoretical description of the image formation process, the best one can do is to use probability density function characterizing empirical data. The commonly used probability density functions (pdfs) for this are Rayleigh^{1,6}, Gamma^{2,3,6}, Weibull^{3,6}, K⁶⁻⁸, Nakagami^{5,6}, and lognormal³. Tao³, *et al.* experimentally evaluated four empirical probability distribution models (Gamma, Weibull, Normal and lognormal) for speckle in clinical cardiac US images and found that the experimental data support a unimodal distribution. They found that Gamma and Weibull distributions are appropriate for characterising blood and tissue. Further the Gamma distribution provides a better overall fit. These authors argue that the empirical distributions considered by them, have the ability to fit gray level densities in blood and tissue regions. However, Tao³, *et al.* pointed out that the significance values for the goodness of fit are not high enough to support the null hypothesis. This motivates us to look for other family of distributions which can model the data better. We explore the Pearson family

of distributions⁹⁻¹² to model the gray level distribution for tissue and blood regions. Author has proposed the Pearson family of distribution for classification of US B-mode kidney images and demonstrated the efficacy of the family over other commonly used distributions. The purpose of this paper is to investigate the applicability of Pearson family to echocardiographic images.

2. THE PEARSON FAMILY OF DISTRIBUTIONS

The richness of Pearson family of distributions is due to the fact that several known distributions viz. Gaussian, beta, Student's t-distributions are contained in the family¹¹. Renzo¹¹, *et al.* noted that the four-parameter Pearson family makes explicit correspondence with the first four moments of the distribution. Pearson⁹ proposed a class of probability density functions (pdfs) which can be generated from the solution of the differential Eqn. (1):

$$\frac{df(x)}{dx} = \left\{ \frac{b+x}{a_0 + a_1x + a_2x^2} \right\} f(x) \quad (1)$$

The random variable X denotes the gray level intensity of the echocardiographic speckle and $f(x)$ represents the probability density function (pdf). The b , a_0 , a_1 , and a_2 are parameters of the distribution. These parameters are determined in terms of the first four central moments (μ_i for $i=1, \dots, 4$) of the underlying empirical distribution. By using method of moments, we have

$$\left\{ \begin{aligned} b = -a_1 &= \frac{0.5\mu_3(3\mu_2^2 + \mu_4)}{9\mu_2^3 - 5\mu_2\mu_4 + 6\mu_3^2} \\ a_0 &= \frac{0.5\mu_2(4\mu_2\mu_4 - 3\mu_3^2)}{9\mu_2^3 - 5\mu_2\mu_4 + 6\mu_3^2} \\ a_2 &= \frac{0.5(6\mu_2^3 - 2\mu_2\mu_4 + 3\mu_3^2)}{9\mu_2^3 - 5\mu_2\mu_4 + 6\mu_3^2} \end{aligned} \right. \quad (2)$$

Pearson⁹ identified a selection parameter κ which is expressible in terms of the first four moments. Defining Skewness ($S_k = \mu_3 / \mu_2^{3/2}$) and Kurtosis ($K_u = \mu_4 / \mu_2^2$), we find

$$\kappa = \frac{S_k^2(K_u + 3)^2}{4(4K_u - 3S_k^2)(2K_u - 3S_k^2 - 6)} \quad (3)$$

The three major types of Pearson densities, i.e. Type I, Type IV and Type VI are defined for $\kappa < 0$, $0 < \kappa < 1$ and $\kappa > 1$, respectively. For the sake of completeness we give the expression of pdfs for three major types.

2.1. Pearson Type I Distribution ($\kappa < 0$)

The pdf of type I distribution is given by

$$f_I(x) = A_0 \left(1 + \frac{x - m_o}{c_1}\right)^{g_1} \left(1 - \frac{x - m_o}{c_2}\right)^{g_2}, \quad -c_1 + m_o < x < c_2 + m_o \quad (4)$$

where

$$\left\{ \begin{aligned} A_0 &= \frac{g_1^{g_1} g_2^{g_2} \Gamma(g_1 + g_2 + 2)}{(c_1 + c_2)(g_1 + g_2)^{g_1 + g_2} \Gamma(g_1 + 1) \Gamma(g_2 + 1)} \\ g_{2,1} &= 0.5h - 1 \pm \text{sign}(\mu_3)(0.5h(h + 2)) \frac{S_k}{\sqrt{S_k^2(h + 2)^2 + 16h + 16}} \\ c_1 &= \left(\frac{g_1}{g_2}\right) \frac{0.5\sqrt{\mu_2\{S_k^2(h + 2)^2 + 16h + 16\}}}{1 + \frac{g_1}{g_2}} \\ c_2 &= 0.5\sqrt{\mu_2\{S_k^2(h + 2)^2 + 16h + 16\}} - c_1 \\ h &= \frac{6K_u - 6S_k^2 - 6}{6 + 3S_k^2 - 2K_u} \\ m_o &= \mu_1 - 0.5 \frac{\mu_3(h + 2)}{\mu_2(h - 2)} \end{aligned} \right. \quad (5)$$

2.1. Pearson Type IV Distribution ($0 < \kappa < 1$)

The pdf of type IV distribution is given by

$$f_{IV}(x) = A_0 \left\{ 1 + \left(\frac{x - m_0}{c_1} \right)^2 \right\}^{-g_1} e^{-\alpha \arctan\left(\frac{x - m_0}{c_1}\right)}, \quad -\infty < x < \infty \quad (6)$$

where

$$\left(\begin{aligned} A_0 &= 0.5\sqrt{2} \sqrt{\frac{h}{\Pi}} e^{\frac{(\cos \theta)^2}{3h} - \frac{1}{12h} - 6\alpha (\cos \theta)^{-h-1}} \\ h &= -\frac{6K_u - 6S_k^2 - 6}{6 + 3S_k^2 - 2K_u} \\ \theta &= \arctan \frac{\alpha}{h} \\ g_1 &= 0.5h + 1 \\ \alpha &= \frac{S_k(-h^2 + 2h)}{\sqrt{(16h - 16) - S_k^2(h - 2)^2}} \\ c &= 0.25\sqrt{\mu_2} \sqrt{(16h - 16) - S_k^2(h - 2)^2} \\ m_0 &= \mu_1 + \frac{\alpha c}{h} \end{aligned} \right) \quad (7)$$

2.1. Pearson Type VI Distribution ($\kappa > 1$)

The pdf of type IV distribution is defined by

$$f_{VI}(x) = A_0(x - m_o - c)^{g_2}(x - m_o)^{-g_1}, \quad c + m_o < x < \infty \quad (8)$$

where

$$\left(\begin{aligned} A_0 &= \frac{c^{(g_1 - g_2 - 1)} \Gamma(g_1)}{\Gamma(g_1 - g_2 - 1) \Gamma(g_2 + 1)} \\ g_1 &= -0.5h + 1 + 0.5h(h + 2) \frac{S_k}{\sqrt{S_k^2(h + 2)^2 + 16h + 16}} \\ g_2 &= 0.5h - 1 + 0.5h(h + 2) \frac{S_k}{\sqrt{S_k^2(h + 2)^2 + 16h + 16}} \\ c &= 0.5\sqrt{\mu_2\{S_k^2(h + 2)^2 + 16h + 16\}} \\ h &= \frac{6K_u - 6S_k^2 - 6}{6 + 3S_k^2 - 2K_u} \\ m_0 &= \mu_1 - \frac{c(g_1 - 1)}{g_1 - g_2 - 2} \end{aligned} \right) \quad (9)$$

3. STATISTICAL CHARACTERISATIONS OF TISSUE AND BLOOD

The images as obtained from GE Voluson 730-Pro ultrasound machine (GE health care systems, New Delhi, India) with frequency range of 3.5 to 5 MHz in respect of 10 clinical echocardiographic B-mode human images with normal status are analyzed. The images are in 8 bit format with 256 gray levels ranging from 0 to 255. For the purpose of illustration we show in Figure 1 the echocardiographic image of subject 1. The dark regions in the image correspond to blood pool whereas the bright portions correspond to tissue. The statistical details of tissue and blood regions are collected by four rectangular windows of M x N pixels. These windows are randomly chosen over the tissue and blood regions in each of 10 B-mode echocardiographic images. The selected tissue regions are shown with blue rectangles (Fig. 1(a)) whereas blood regions with red rectangles

(Fig. 1(b)). These regions are marked with 1–4 and referred to as T_1 - T_4 (for tissue) and B_1 - B_4 (for blood). The collected data from Figs. 1(a)-(b) are represented as histograms (Figs. 2-3).

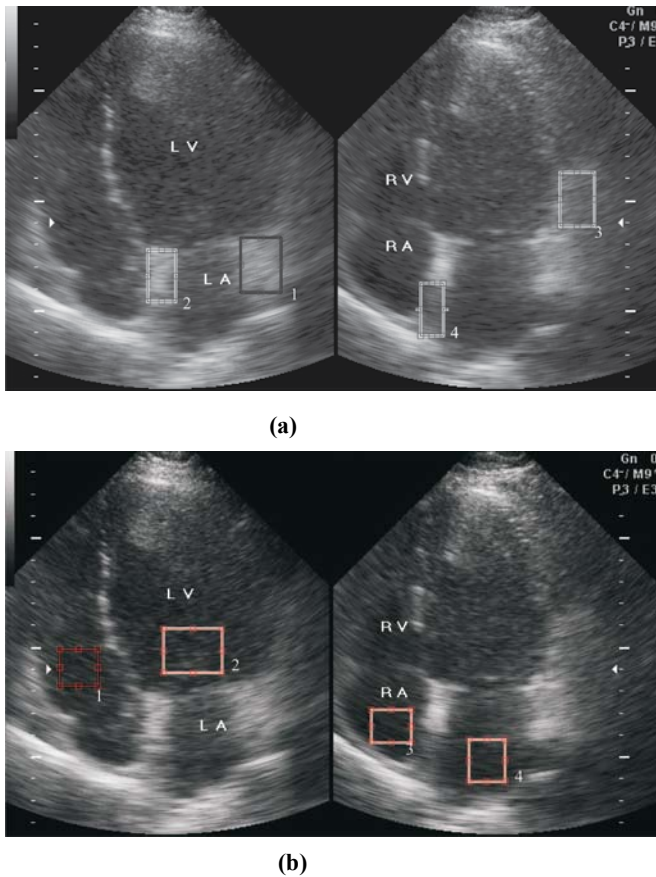


Figure 1. B-Mode echocardiographic image with regions of interests (ROI) (a) Blue rectangles represent four tissue regions (T_1 - T_4) (b) Red rectangles represent four blood regions (B_1 - B_4).

3.1 Fitting of Pearson Distributions

The aim of our investigation is to identify plausible Pearson type for gray level distributions of tissue and blood. With advice from expert radiologist, we have manually identified four rectangular regions corresponding to tissue and four rectangular regions corresponding to blood. Thus from 10 images we have data for 40 regions for each of tissue and blood. In tissue regions the number of pixels under rectangular window varies from 952 to 2575 whereas in blood regions it varies from 860 to 2744. The data (gray values) collected from each region are divided into a set of 10 bins. The selection parameter κ is computed for each image form first four moments as given in Eqn. 3. MATLAB (Mathworks) 7.5.0.342 (R2007b) software is used for estimation of parameters. The computed κ values for T_1 - T_3 , B_2 and B_4 regions turn out to be negative, the selected Pearson distributions would thus correspond to Type I distribution. Using Eqn. 5 parameters for this pdf are obtained and are given in Table 1. For regions T_4 , B_1 and B_3 , computed κ values

are positive and less than unity which corresponds to Type IV Pearson distribution. Parameters for this pdf as obtained by using set of Eqns. 8 are given in Table 2. By employing Eqns. (4) and (6), the pdfs for these regions are obtained and are plotted in Figs. 2-3 against their respective histograms. These pdfs are found to be in excellent agreement with the empirical data.

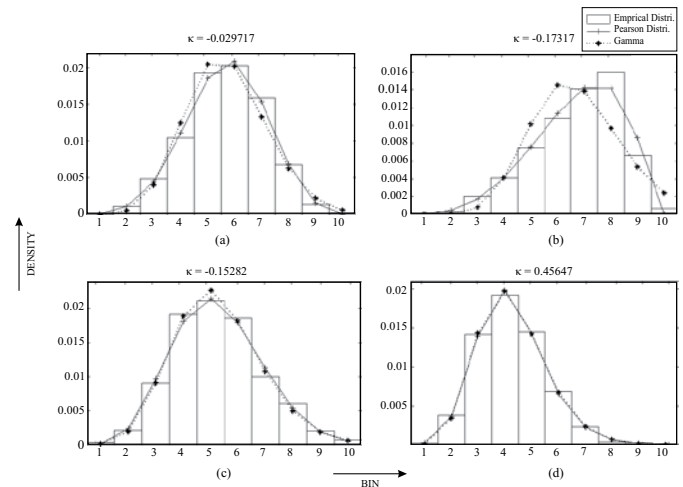


Figure 2 (a-d).Characterisation of gray level distribution in tissues (T_1 - T_4) of B-Mode echocardiographic images (ROI in Fig.1(a)) by employing Pearson Family and Gamma distributions.

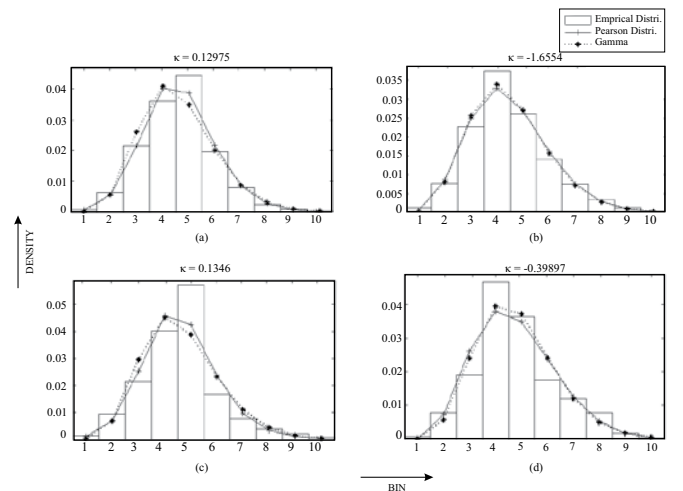


Figure 3 (a-d). Characterisation of gray level distribution in blood (B_1 - B_4) of B-Mode echocardiographic images (ROI in Fig. 1(b)) by employing Pearson Family and Gamma distributions.

The κ based Characterization and resulting Pearson type for 40 tissue and blood regions in 10 echocardiographic images is summarized in Table 3. It can be seen from Table 3 that in most cases the Pearson type I distribution characterises tissue and blood. To test the efficacy of Pearson⁹ over Gamma³ distribution, we are required to fit Gamma distribution to the data sets generated from the echocardiographic images. The parameters of Gamma³ distribution are obtained by employing the maximum likelihood estimation approach and these are given in Table 4. The pdfs of Gamma³ distribution for

these parameters are plotted in Figs. 2-3 and the fit of Gamma distribution to the real data set is fairly good. It is interesting to note that the results based on Gamma distribution in Table 4 indicates lower β corresponds to blood whereas higher β captures the characteristics of tissues. To compare the effectiveness of Pearson⁹ versus Gamma³, we calculate statistical measures viz. JS¹⁴ divergence and KS² test which are discussed in subsequent section.

4. GOODNESS OF FIT TESTS

To facilitate the comparison of Pearson versus Gamma with respect to empirical data, we need a measure of distance between probability distributions. Here we consider two such measures.

4.1 Jensen-Shannon Divergence

To this end one of the widely used measures is based on Kullback- Leibler¹³(KL) divergence. The KL¹³ measure defines distance of probability distribution

$P = \{p_1, p_2, \dots, p_n\}$ from a reference distribution $Q = \{q_1, q_2, \dots, q_n\}$ as

$$D(P \parallel Q) = \sum_{i=1}^n p_i \log \frac{p_i}{q_i} \tag{10}$$

Since $D(P \parallel Q) \neq D(Q \parallel P)$, reflecting the asymmetric nature of KL¹⁴ measure, one can obtain a symmetric measure known as JS divergence¹⁴. We have

$$JS(P, Q) = \frac{D(P \parallel \frac{(P+Q)}{2}) + D(Q \parallel \frac{(P+Q)}{2})}{2} \tag{11}$$

JS divergence¹⁴ is based on information theory. Another well known distance measure commonly adopted for study of goodness of fit is based on Kolmogorov-Smirnov^{2,6} (KS) test.

4.2 Kolmogorov-Smirnov Test

The distance between the cumulative distribution function (cdf) of random variable X with empirical data

Table 1. Parameter values of Type I Pearson distribution for ROIs in Fig. 1

Region	κ	A_0	g_1	g_2	h	c_1	c_2	m_0
T ₁	-0.02972	0.26167	16.21874	11.21801	29.43675	9.85770	6.81827	9.60828
T ₂	-0.17317	0.23714	3.73646	1.10716	6.84362	7.58545	2.24765	8.80615
T ₃	-0.15282	0.24082	5.75727	13.49511	21.25239	4.91343	11.51713	6.97713
B ₂	-1.65540	0.27030	7.36597	70.14413	79.51010	4.21673	40.15478	4.22526
B ₄	-0.39897	0.25581	3.95830	15.32330	21.28160	3.58084	13.86210	4.76602

Table 2. Parameter values of Type IV Pearson distribution for ROIs in Fig. 1

Region	κ	A_0	h	θ	g_1	α	c	m_0
T ₄	0.45647	0.00002	26.80793	-0.74181	14.40396	-24.56708	4.91338	0.11552
B ₁	0.12975	0.08938	18.54003	-0.36849	10.27002	-7.15886	5.40235	2.66211
B ₃	0.13460	0.13367	12.19587	-0.37565	7.09793	-4.80979	4.51698	2.79586

Table 3. Occurrences of different Pearson Types in 40 tissue and blood regions

Region	Type I	Type IV	Type VI
Tissue	39	1	0
Blood	27	10	3

Table 4. Parameter values of Gamma³ distribution for ROIs in Fig. 1

Parameter	Region							
	T ₁	T ₂	T ₃	T ₄	B ₁	B ₂	B ₃	B ₄
β	39.875	22.252	20.825	12.907	11.130	9.749	9.709	11.992
λ	2.973	5.805	3.928	5.821	3.013	3.939	2.949	2.941

can be defined as

$$D = \max |P_{empirical}(X \leq x) - P_{reference}(X \leq x)| \quad (12)$$

The goodness of fit requires comparison of D to a critical level D_{max} (for details see Raju⁶, *et al.*). A smaller value of the $KS^{2,6}$ statistics indicates a better fit of the empirical distribution to that of reference distribution.

5. RESULTS

We describe the results of statistical measures for testing goodness of fit in respect of Pearson and Gamma distributions with empirical distribution. To this end we consider the image of subject 1 with four tissue and four blood regions. We give in Table 5, the results of JS^{14} (Eqn. 11) and $KS^{2,6}$ (Eqn. 12) statistics for tissue (T_{1-4}) and blood (B_{1-4}) regions with regard to Pearson and Gamma distribution. The bold numerical values in Table 5 show the efficacy of corresponding distribution. It can be easily seen that Pearson family outperforms over Gamma distribution.

Table 5. JS Divergence and KS Test results for distributions in Figs 2-3 wrt empirical distribution

Region	$JS_{Pearson}$	JS_{Gamma}	$KS_{Pearson}$	KS_{Gamma}
T_1	0.00034	0.00390	0.00516	0.02050
T_2	0.00535	0.01835	0.01985	0.07791
T_3	0.00093	0.00083	0.00792	0.01184
T_4	0.00078	0.00117	0.00557	0.00800
B_1	0.00151	0.00457	0.02339	0.05443
B_2	0.00189	0.00214	0.02099	0.01911
B_3	0.00803	0.01329	0.04908	0.05895
B_4	0.00702	0.00606	0.04010	0.03248

The results of all images (40 blood regions and 40 tissue regions) taken together, are summarized in Table 6. From this table it is noted that the success counts in respect of Pearson distributions is far more than that of Gamma distribution.

6. CONCLUSIONS

The Characterisation of blood and tissue in echocardiographic images is very important in medical applications. The problem of Characterisation from first principles is fairly complicated. Consequently, the research investigations adopt statistical framework for modeling the distributions of gray level densities in tissue and blood. Typically unimodal distributions such as Rayleigh, Gamma, Weibull, K, Nakagami, and Lognormal have been used for this. Tao³, *et al.* in a recent paper pointed out that the choice of these distributions does not lead to the desired significance level to support the null hypothesis. This demand for the investigation to identify some appropriate probability distributions. Motivated by the success of Pearson family in wireless communication¹⁰⁻¹², we have investigated its applicability in medical imaging. We have demonstrated the efficacy of Pearson family of distributions over Gamma distribution in echocardiography. A useful area of future enquiry would be to investigate in future the utility of model parameters as well the first four moments for characterisation of medical images.

ACKNOWLEDGEMENT

The authors are grateful to Professor N. R. Pal (Indian Statistical Institute, Kolkata) whose valuable suggestions have improved the contents and quality of the paper. Author would like to thank Dr Yogesh Sharma, Radiologist, Noida Diagnostic Center for getting the approval of the ethics committee of the hospital for use of medical images in the research.

Table 6. Success of Pearson and Gamma distributions in 40 tissue and 40 blood regions based on JS divergence and KS test

		JS Divergence				KS Test			
		Pearson wins	Gamma wins	% success Pearson	% success Gamma	Pearson wins	Gamma wins	% success Pearson	% success Gamma
Tissue	Type I versus Gamma	34	5	87.18	12.82	37	2	94.87	5.13
	Type IV versus Gamma	1	0	100.00	0	1	0	100.00	0
	Type I versus Gamma	17	10	62.96	37.04	17	10	62.96	37.04
Blood	Type IV versus Gamma	9	1	90.00	10.00	9	1	90.00	10.00
	Type VI versus Gamma	2	1	66.67	33.33	1	2	33.33	66.67

REFERENCE

1. Wagner, R.F.; Smith, S.W.; Sandrik J.M. & Lopez, H. Statistics of speckle in ultrasound B-scans. *IEEE Trans. Ultra. Ferro. Freq. Control*, 1983, **30**(3), 156-63.
2. Nillesen, M.N.; Lopata, R.G.P.; Gerrits, I.H.; Kapusta, L.; Thijssen, J.M. & Korte, C.L.D. Modeling envelope statistics of blood and myocardium for segmentation of echocardiographic images. *Ultrasound Med. Biol.*, 2008, **34**(4), 674-80.
3. Tao, Z.; Tagare, H.D. & Beaty, J. D. Evaluation of four probability distribution models for speckle in clinical cardiac ultrasound images. *IEEE Trans Med. Imag.*, 2006, **25**(11), 1483-1491.
4. Mittal, D.; Kumar, V.; Saxena, S.C.; Khandelwal, N. & Kalra, N. Enhancement of the ultrasound images by modified anisotropic diffusion method. *Med. Biol. Eng. Comput.*, 2010, **48**, 1281-291.
5. Shankar, P.M.; Dumane, V.A.; Reid, J.M.; Genis, V.; Forsberg, F.; Piccoli, C.W. & Goldberg, B.B. Classification of ultrasonic B-mode images of breast masses using Nakagami distribution. *IEEE Trans. Ultra. Ferro. Freq. Control*, 2001, **48**(9), 569-80.
6. Raju, B.I. & Srinivasan M.A. Statistics of envelope of high frequency ultrasonic backscatter from human skin in vivo. *IEEE Trans. Ultra. Ferro. Freq. Control*, 2002, **49**(7), 871-82.
7. Bernard, O.; D'hooge, J. & Friboulet, D. Statistics of the radio frequency signal based on K distribution with application to echocardiography. *IEEE Trans. Ultra. Ferro. Freq. Control*, 2006, **53**(9), 1689-694.
8. Bernard, O.; Touil, B.; D'hooge, J. & Friboulet, D. Statistical modeling of the radio-frequency signal for partially- and fully-developed speckle based on a generalized Gaussian model with application to echocardiography. *IEEE Trans. Ultra. Ferro. Freq. Control.*, 2007, **54**(10), 2189-194.
9. Elderton, W.P. & Johnson, N.L. System of frequency curves. London, Cambridge University Press, 1969.
10. Kwan, R. & Leung, C. On the applicability of the pearson method for approximating distributions in wireless communications. *IEEE Trans. Comm.*, 2007, **55**(11), 2065-069.
11. Renzo, M.D.; Graziosi, F. & Santucci, F. Approximating the linear combination of log-normal RVs via pearson type IV distribution for UWB performance analysis. *IEEE Trans. Comm.*, 2009, **57**(2), 388-403.
12. Zhang, Q.T. & Song, S.H. A systematic procedure for accurately approximating lognormal-sum distributions. *IEEE Trans. Vehicular Technol.*, 2008, **57**(1), 663-66.
13. Entropy measures, maximum entropy principle and emerging applications, *edited by* Karmeshu. Germany, Springer-Verlag, 2003.
14. Lin, J. Divergence measures based on the Shannon entropy. *IEEE Trans. Infor. Theory*, 1991, **37** (1), 145-51.

Contributors



Mr Abhinav Gupta received BTech (Electrical Engg.) from I.E.T., M.J.P. Rohilkhand University, Bareilly and MTech (Signal Processing) from I.I.T. Guwahati. He is pursuing his PhD at the School of Computer and Systems Sciences, Jawaharlal Nehru University, New Delhi. Presently working as a Senior Lecturer in Department Electronics and Communication Engineering, Jaypee

Institute of Information Technology, Noida.



Dr Karmeshu has been working as Professor in School of Computer and System Sciences, Jawaharlal Nehru University, New Delhi, India, since 1986. In 1993, he received the Shanti Swarup Bhatnagar Award, India's most prestigious award in the field of science and engineering, for his contributions to mathematical modeling of social and technical systems. He has published

about 100 papers in journals. His current research interests includes: Wireless systems, bio-informatics/computational neuroscience and medical imaging.